Al- Khwarizmi Engineering Journal

Al- Khwarizmi Engineering Journal Vol. 3 , , No. 1, pp63 – ٩٣ (2007)

Laminar Natural Convection of Newtonian and Non – Newtonian Fluids Inside Triangular Enclosure

Dr. Ala'a Abbas Muhadi
Mech. Eng. Dept.
University of Kufa
(Received 31 July 2006 ; accepted 19 December 2006)

Abstract

In the present work, steady two – dimensional laminar natural convection heat transfer of Newtonian and non-Newtonian fluids inside isosceles triangular enclosure has been analyzed numerically for a wide range of the modified Rayleigh numbers of ($10^3 \leq Ra \leq 10^5$), with non-dimensional parameter (*NE*) of Prandtl – Eyring model ranging from (0 to 10), and modified Prandtl number take in the range (Pr^* =1,10, and 100). Two types of boundary conditions have been considered. The first, when the inclined walls are heated with different uniform temperatures and the lower wall is insulated. The second, when the bottom wall is heated by applying a uniform heat flux while the inclined walls at the constant cold temperature. Also, the non-Newtonian fluids under consideration were assumed to obey the Prandtl – Eyring model. The results are presented in terms of isotherms and streamlines to show the behavior of the fluid flow and temperature fields. In addition, some graphics are presented the relation between average Nusselt number and the various parameters. The results show the effect of non – dimensional parameter (*NE*) on the velocity and temperature profiles. They also show that the average Nusselt number is a strong function of modified Rayleigh number, modified Prandtl number, non-dimensional parameter, and the boundary conditions. Four different correlations have been made to show the dependence of the average Nusselt number on the non-dimensional parameter, the modified Rayleigh and Prandtl numbers.

Keywords: Natural Convection – Non-Newtonian Fluids – Triangular Enclosures - Finite Differences Method.

Nomenclature

A & B : Fluid consistency indices for the Prandtl – Eyring model ($kg/m.s^2$) & (s)

g : Gravitational acceleration (m/s^2).

h : Heat transfer coefficient ($W/m^2.K$).

k : Thermal conductivity of fluid ($W/m.K$).

L : Width and Height of enclosure (m).

L_c : Length of the inclined wall (m).

NE : Fluid index of Prandtl – Eyring model $= \dfrac{\alpha B}{L^2}$.

Nu : Nusselt number $= \dfrac{qL}{k(T_h - T_c)}$.

Nu_a : Average Nusselt number.

P : Pressure (Pa).

Pr : Prandtl number = (υ/α).

Pr^* : Modified Prandtl number $= \dfrac{AB}{\rho_o \alpha}$.

q : Heat flux (W/m^2).

Ra : Modified Rayleigh number

$$= \begin{cases} Ra_E = \dfrac{\rho_o g \beta L^3 (T_h - T_c)}{AB\alpha} & \textbf{for B.C.1} \\ Ra_E^* = Ra_E Nu = \dfrac{\rho_o g \beta L^4 q}{AB\,\alpha k} & \textbf{for B.C.2} \end{cases}$$

T : Temperature (K).

u : Fluid velocity in x-direction (m/s).

v : Fluid velocity in y-direction (m/s).

x& y : Cartesian coordinates.

Greek Symbols

α : Thermal diffusivity (m^2/s).

β : Thermal expansion coefficient ($1/K$).

f : Any arbitrary function, $f(x,y)$.

ΔT : Temperature difference (K).

Δx & Δy : Regular grid size in the x and y directions, respectively (m).

Δx_r & Δy_r : Irregular grid size in the x and y directions, respectively (m).

θ : Dimensionless temperature

$$= \begin{cases} \dfrac{T - T_c}{T_h - T_c} & \textbf{for B.C.1} \\ \dfrac{T - T_c}{\dfrac{qL}{k}} & \textbf{for B.C.2} \end{cases}$$

μ : Dynamic viscosity, ($kg/m.s$).

υ : Kinematic viscosity of fluid (m^2/s).

ρ : Density (kg/m^3).

τ_{xx} : Normal stress in the x direction.

τ_{yx} : Shear stress (Pa) =

$$\begin{cases} \mu \dfrac{\partial u}{\partial y} \; for Newtonian Fluid \\ A \sinh^{-1}\left(B \dfrac{\partial u}{\partial y}\right) for non - Newtonian Fluid \end{cases}$$

τ_{yy} : Normal stress in the y direction.

ψ : Stream function (m^2/s).

ω : Vorticity ($1/s$).

1. Introduction

Natural convection in enclosures, has been extensively studied due to it's wide ranging applications such as building insulation, solar cavity receivers, ventilation of rooms, storage of grease, mineral oil, or crude oil in containers, nuclear reactor insulation, crystal growth in liquids, and the cooling of electrical components [1]. However, the efforts have been mainly directed toward the investigation of convection in rectangular enclosures, which may be leveled or tilted. Relatively, very little

attention is focused on the study of natural convection in triangular enclosures. In the present work, a numerical study is performed to analyze the natural convection heat transfer of Newtonian and non – Newtonian fluids inside triangular enclosure under two different cases of boundary conditions. The fluid motion and heat transfer are affected by modified Rayleigh number, modified Prandtl number, and non – dimensional parameter (*NE*) of Prandtl – Eyring model. The non – dimensional parameter (*NE*) determines the nature of fluid, that is, Newtonian (*NE* = 0) and non – Newtonian fluids (*NE* > 0). The mass, momentum, and energy conservation equations, which are considered to describe the fluid flow and heat transfer for natural convection are nonlinear and because of this non linearity, some difficulties have arisen in numerical as well as in analytical studies [2]. One of the greatest difficulties with the numerical studies is the problem of divergence of the iterative methods since an analytical solution of the actual problem is extremely difficult, if not possible, a number of assumptions together with the computational fluid dynamic techniques are used to obtain approximate results [3].

2. Mathematical Formulation :-

The schematic of the physical model and the coordinate system are shown in Fig.(1). It is isosceles triangular region of width (*L*) and height (*L*) under two different cases of thermal boundary conditions, these boundary conditions are:

Case(I) :-

The inclined walls are heated with different uniform temperatures (T_h & T_c) and the lower wall is perfectly insulated (B.C.1), as shown in (Fig.1a).

Case(II) :-

The lower wall is heated by applying a uniform heat flux (q) and the inclined walls are isothermally cooled (T_c) (B.C.2), as shown in (Fig.1b). Density is also considered as constant value but for buoyant term it is linearised by relation:

$$\rho = \rho_o[1-\beta(T-T_o)] \quad (1)$$

were β is thermal expansion coefficient for temperature T_o.

The depth of the region is assumed to be sufficiently large so that the flow and the heat transfer are two dimensional. The fluid considered is non – Newtonian and the flow laminar. For the present physical model, subject to the Boussinesque approximation, the governing equations in their primitive form, are given by:

$$\frac{\partial u}{\partial x}+\frac{\partial v}{\partial y}=0 \quad (2)$$

$$\rho_o\left(u\frac{\partial u}{\partial x}+v\frac{\partial u}{\partial y}\right)=-\frac{\partial p}{\partial x}+\frac{\partial \tau_{xx}}{\partial x}+\frac{\partial \tau_{yx}}{\partial y} \quad (3)$$

$$\rho_o\left(u\frac{\partial v}{\partial x}+v\frac{\partial v}{\partial y}\right)=-\frac{\partial p}{\partial y}+\frac{\partial \tau_{xy}}{\partial x}+\frac{\partial \tau_{yy}}{\partial y}-\rho g \quad (4)$$

$$u\frac{\partial T}{\partial x}+v\frac{\partial T}{\partial y}=\alpha\left(\frac{\partial^2 T}{\partial x^2}+\frac{\partial^2 T}{\partial y^2}\right) \quad (5)$$

In the above equations, (u, v, α, P, T) are the fluid velocity components, the thermal diffusivity, the pressure and the temperature. In fact Eqs.(2 to 5) are system of partial differential equations. They are the base for natural convection phenomenon for 2D

enclosures, presented by mass, momentum and energy conservation equations. As was mentioned in Ref.[4], the Prandtl – Eyring model for non – Newtonian fluids can be represented as:

$$\tau = A\,sinh^{-1}(B\frac{\partial u}{\partial y}) \qquad (6)$$

Hence, the shear stresses:

$$\tau_{xx} = 2A\,sinh^{-1}(B\frac{\partial u}{\partial x}) \qquad (7)$$

$$\tau_{yy} = 2A\,sinh^{-1}(B\frac{\partial v}{\partial y}) \qquad (8)$$

$$\tau_{xy} = \tau_{yx} = A\,sinh^{-1}[B(\frac{\partial u}{\partial y} + \frac{\partial v}{\partial x})] \qquad (9)$$

where A and B are the fluid consistency indices for the Prandtl – Eyring model.

Since it proves to be more convenient to work in terms of a stream function and vorticity, the stream function $\psi(x,y)$ is introduced in the usual manner:

$$u = \frac{\partial \psi}{\partial y} \quad \& \quad v = -\frac{\partial \psi}{\partial x} \qquad (10)$$

It is evident from Eq.(10) that the stream function satisfies the continuity equation identically. Further more, for this plane flow field, the only non – zero component of the vorticity is:

$$\omega = \frac{\partial v}{\partial x} - \frac{\partial u}{\partial y} \qquad (11)$$

Combining the definition of vorticity and the velocity components in terms of the stream function, and cross – differentiating the Eqs.(3) and (4) to reduce the number of equations and eliminate the pressure terms, and substituting for (ρ) from Eq.(1), a new set of equations is obtained with independent variables ψ, ω and T:

$$\frac{\partial^2 \psi}{\partial x^2} + \frac{\partial^2 \psi}{\partial y^2} = -\omega \qquad (12)$$

$$\rho_o[\frac{\partial \psi}{\partial y}\frac{\partial \omega}{\partial x} - \frac{\partial \psi}{\partial x}\frac{\partial \omega}{\partial y}] = AB[\frac{\partial^2 \omega}{\partial x^2} + \frac{\partial^2 \omega}{\partial y^2}]$$
$$+ AB[\frac{\partial S_1}{\partial x} - \frac{\partial S_2}{\partial y} - 4\frac{\partial S_3}{\partial x}] + S_G \qquad (13)$$

$$\frac{\partial \psi}{\partial y}\frac{\partial T}{\partial x} - \frac{\partial \psi}{\partial x}\frac{\partial T}{\partial y} = \alpha(\frac{\partial^2 T}{\partial x^2} + \frac{\partial^2 T}{\partial y^2}) \qquad (14)$$

$$S_G = AB[\frac{\partial^4 \psi}{\partial x^4} + \frac{\partial^4 \psi}{\partial y^4} + 2\frac{\partial^4 \psi}{\partial x^2 \partial y^2}] \,,,$$
$$+ \rho_o g\beta \frac{\partial T}{\partial x} \qquad (15)$$

$$S_1 = \frac{\frac{\partial^3 \psi}{\partial x \partial y^2} - \frac{\partial^3 \psi}{\partial x^3}}{\sqrt{1 + (B(\frac{\partial^2 \psi}{\partial y^2} - \frac{\partial^2 \psi}{\partial x^2}))^2}},$$

$$S_2 = \frac{\frac{\partial^3 \psi}{\partial y^3} - \frac{\partial^3 \psi}{\partial y \partial x^2}}{\sqrt{1 + (B(\frac{\partial^2 \psi}{\partial y^2} - \frac{\partial^2 \psi}{\partial x^2}))^2}}, \quad \&$$

$$S_3 = \frac{\frac{\partial^3 \psi}{\partial x \partial y^2}}{\sqrt{1 + (B\frac{\partial^2 \psi}{\partial x \partial y})^2}} \qquad (16)$$

Now, The mathematical problem formulated above was placed in dimensionless form by defining the new dimensionless variables [5]:

$$x^* = \frac{x}{L} \;,\; y^* = \frac{y}{L}$$

$$\theta = \begin{cases} \dfrac{T - T_c}{T_h - T_c} & \text{for B.C.1} \\ \dfrac{T - T_c}{\frac{qL}{k}} & \text{for B.C.2} \end{cases}$$

$$\psi^* = \frac{\psi}{\alpha} \;,\; \omega^* = \frac{\omega L^2}{\alpha}$$

Inserting all the dimensionless variables into Eqs.(12) to (16), yield the following final non – dimensional equations:

$$\frac{\partial^2\psi^*}{\partial x^{*2}}+\frac{\partial^2\psi^*}{\partial y^{*2}}=-\omega^* \qquad (17)$$

$$\frac{\partial\psi^*}{\partial y^*}\frac{\partial\omega^*}{\partial x^*}-\frac{\partial\psi^*}{\partial x^*}\frac{\partial\omega^*}{\partial y^*}=\Pr^*\left[\frac{\partial^2\omega^*}{\partial x^{*2}}+\frac{\partial^2\omega^*}{\partial y^{*2}}\right]+\Pr^*\left[\frac{\partial S_1^*}{\partial x^*}-\frac{\partial S_2^*}{\partial y^*}-4\frac{\partial S_3^*}{\partial x^*}\right]+S_G^* \qquad (18)$$

$$\frac{\partial\psi^*}{\partial y^*}\frac{\partial\theta}{\partial x^*}-\frac{\partial\psi^*}{\partial x^*}\frac{\partial\theta}{\partial y^*}=\frac{\partial^2\theta}{\partial x^{*2}}+\frac{\partial^2\theta}{\partial y^{*2}} \qquad (19)$$

where;

$$S_G^*=\Pr^*\left[\frac{\partial^4\psi^*}{\partial x^{*4}}+\frac{\partial^4\psi^*}{\partial y^{*4}}+2\frac{\partial^4\psi^*}{\partial x^{*2}\partial y^{*2}}\right]+\Pr^*Ra\frac{\partial\theta}{\partial x^*} \qquad (20)$$

$$S_1^*=\frac{\frac{\partial^3\psi^*}{\partial x^*\partial y^{*2}}-\frac{\partial^3\psi^*}{\partial x^{*3}}}{\sqrt{1+\left(NE\left(\frac{\partial^2\psi^*}{\partial y^{*2}}-\frac{\partial^2\psi^*}{\partial x^{*2}}\right)\right)^2}} \qquad (21)$$

$$S_2^*=\frac{\frac{\partial^3\psi^*}{\partial y^{*3}}-\frac{\partial^3\psi^*}{\partial y^*\partial x^{*2}}}{\sqrt{1+\left(NE\left(\frac{\partial^2\psi^*}{\partial y^{*2}}-\frac{\partial^2\psi^*}{\partial x^{*2}}\right)\right)^2}} \qquad (22)$$

$$S_3^*=\frac{\frac{\partial^3\psi^*}{\partial x^*\partial y^{*2}}}{\sqrt{1+\left(NE\left(\frac{\partial^2\psi^*}{\partial x^*\partial y^*}\right)\right)^2}} \qquad (23)$$

$Pr^*=\frac{AB}{\rho_o\,\alpha}$ is the modified Prandtl number.

$$Ra=\begin{cases}Ra_E=\dfrac{\rho_o g\beta L^3(T_h-T_c)}{AB\alpha}\\ \textbf{is the modified Rayleigh number for B.C.1}\\ Ra_E^*=Ra_E\,Nu=\dfrac{\rho_o g\beta L^4 q}{AB\,\alpha k}\\ \textbf{is the modified Rayleigh number for B.C.2}\end{cases}$$

$NE=\frac{\alpha B}{L^2}$ is the non- dimensional parameter of Prandtl – Eyring model.

The physical quantities of interest in this problem are the local Nusselt number along the heated wall [6], defined by:

$$Nu=\frac{qL}{k(T_h-T_c)} \qquad (24)$$

and also the average Nusselt number, which is defined as:

Case (I) :-

$$Nu_a=\int_0^{1.118}\sqrt{\left(\frac{\partial\theta}{\partial x^*}\right)^2+\left(\frac{\partial\theta}{\partial y^*}\right)^2}\Bigg|_{x^*=\frac{y^*}{2}\ or\ 1+\frac{y^*}{2}}dc$$

where $dc=\sqrt{(dx_r)^2+(dy_r)^2}$ (25)

Case (II) :-

$$Nu_a=\int_0^1\frac{1}{\theta_h}\Bigg|_{y^*=0}dx \qquad (26)$$

3. Numerical Method :

Numerical methods have been developed to handle problems involving nonlinearities in the describing equations, or complex geometries involving complicated boundary conditions. A non-uniform finite-difference technique is applied to solve the governing equations. These three equations (Eqs.(17), (18), and (19)) are to be solved in a given region subject to the condition that the values of the stream function, temperature, and the vorticity, or their derivatives, are prescribed on the boundary of the domain. The finite difference approximation of the governing equations was based on dividing the $(0\le x^*\le 1)$ interval into (m) equal

segments separated by (m+1) nodes. Likewise, the (y^*) interval was divided into (n) segments, regular and irregular meshes are result as shown in Figs.(3 & 4). Regular mesh has been covered most the triangular region except for the region near from the inclined wall, which was covered with irregular mesh. Assume that unknown variable $f(x,y)$ possesses continuous derivatives, so the approximation of second derivative of (f) to determine interior point are [2]:

$$(\frac{\partial^2 f}{\partial x^2})_{i,j} = \frac{f_{i+1,j} - (a+1)f_{i,j} + af_{i-1,j}}{0.5(\Delta x^2 + a\Delta x_r^2)}$$

and the first derivative central difference are:

$$(\frac{\partial f}{\partial x})_{i,j} = \frac{f_{i+1,j} + (a^2-1)f_{i,j} - a^2 f_{i-1,j}}{\Delta x + a^2 \Delta x_r}$$

where, (a) and (b) are factors representing the degree of non – uniformity and the values of these factors equal to (1) for regular mesh, and calculated from equation of line for irregular mesh. And;

$$\begin{aligned} \Delta x_r &= a\Delta x \\ \Delta y_r &= b\Delta y \end{aligned} \quad \text{if} \quad \begin{aligned} a &\le 1 \\ b &\le 1 \end{aligned}$$

$$\begin{aligned} \Delta x_r &= \frac{\Delta x}{a} \\ \Delta y_r &= \frac{\Delta y}{b} \end{aligned} \quad \text{if} \quad \begin{aligned} a &> 1 \\ b &> 1 \end{aligned}$$

The usual procedure for obtaining the form of partial differential equation with non - uniform finite-difference method [7] is to approximate all the partial derivatives in the equation by means of their Taylor series expansions. Eq.(17) can be approximated using central – difference at the representative interior point (i,j), thus, Eq.(17) can be written for regular mesh as:

$$\psi_{i,j}^* = [(\psi_{i+1,j}^* + a\psi_{i-1,j}^*)(\Delta y^2 + b\Delta y_r^2) + (\psi_{i,j+1}^* + b\psi_{i,j-1}^*)(\Delta x^2 + a\Delta x_r^2) + 0.5(\Delta x^2 + a\Delta x_r^2)(\Delta y^2 + b\Delta y_r^2)\omega_{i,j}^*] /[(a+1)(\Delta y^2 + b\Delta y_r^2) + (b+1)(\Delta x^2 + a\Delta x_r^2)] \quad (27)$$

Also, a central – difference formulation can be used for Eqs.(18), and (19). But this problem will need to be solved for reasonably high values of modified Rayleigh numbers; it is known that such a formulation may not be satisfactory owing to the loss of diagonal dominance in the sets of difference equations, with resulting difficulties in convergence when using an iterative procedure.

A forward – backward technique can be introduced to maintain the diagonal dominance coefficient of ($\omega_{i,j}$) in Eq.(18) and ($\theta_{i,j}$) in Eq.(19) which determines the main diagonal elements of the resulting linear system; this technique is outlined as follows [8]:

Set;

$$\gamma = \psi_{i+1,j}^* + (a^2-1)\psi_{i,j}^* - a^2\psi_{i-1,j}^*$$

and

$$\beta = \psi_{i,j+1}^* + (b^2-1)\psi_{i,j}^* - b^2\psi_{i,j-1}^*$$

Then approximate Eq.(18) by:

$$-0.5((a+1)(\Delta y^2 + b\Delta y_r^2) + (b+1)(\Delta x^2 + a\Delta x_r^2))\omega_{i,j}^* + 0.5Pr^*((\Delta y^2 + b\Delta y_r^2)(\omega_{i+1,j}^* + a\omega_{i-1,j}^*) + (\Delta x^2 + a\Delta x_r^2)(\omega_{i,j+1}^* + b\omega_{i,j-1}^*)) + 0.25(\Delta x^2 + a\Delta x_r^2)(\Delta y^2 + b\Delta y_r^2)[Pr^*(\frac{\partial S_1^*}{\partial x^*} - \frac{\partial S_2^*}{\partial y^*} - 4\frac{\partial S_3^*}{\partial x^*}) + S_G^* + (\frac{\gamma}{\Delta x^2 + a\Delta x_r^2}\frac{\partial \omega^*}{\partial y^*} - \frac{\beta}{\Delta y^2 + b\Delta y_r^2}\frac{\partial \omega^*}{\partial x^*})] = 0 \quad (28)$$

and Eq.(19) by:

$$-0.5((a+1)(\Delta y^2+b\Delta y_r^2)+(b+1)(\Delta x^2+a\Delta x_r^2))\theta_{i,j}$$
$$+0.5((\Delta y^2+b\Delta y_r^2)(\theta_{i+1,j}+a\theta_{i-1,j})+(\Delta x^2+a\Delta x_r^2)$$
$$(\theta_{i,j+1}+b\theta_{i,j-1}))+0.25(\Delta x^2+a\Delta x_r^2)(\Delta y^2+b\Delta y_r^2)$$
$$[\frac{\gamma}{\Delta x^2+a\Delta x_r^2}\frac{\partial\theta}{\partial y^*}-\frac{\beta}{\Delta y^2+b\Delta y_r^2}\frac{\partial\theta}{\partial x^*}]=0 \qquad (29)$$

Now, if

$$\gamma\geq 0,\ \frac{\partial f}{\partial y}=\frac{f_{i,j+1}-f_{i,j}}{\Delta y},\ (b_1=1),\ \textbf{and}\ (b_2=0)$$
$$\gamma<0,\ \frac{\partial f}{\partial y}=\frac{f_{i,j}-f_{i,j-1}}{\Delta y_r},\ (b_1=0),\ \textbf{and}\ (b_2=1)$$
$$\beta\geq 0,\ \frac{\partial f}{\partial x}=\frac{f_{i,j}-f_{i-1,j}}{\Delta x_r},\ (a_1=1),\ \textbf{and}\ (a_2=0)$$
$$\beta<0,\ \frac{\partial f}{\partial x}=\frac{f_{i+1,j}-f_{i,j}}{\Delta x},\ (a_1=0),\ \textbf{and}\ (a_2=1)$$

To assure the diagonal dominance of the coefficient matrix for $(\omega_{i,j}^*)$ **and** $(\theta_{i,j})$, which depends on the sign of (γ) and (β), Eqs.(18) and (19) are expressed in the following difference forms:

$$\omega_{i,j}^*=[(0.25\gamma b_1\frac{(\Delta x^2+a\Delta x_r^2)(\Delta y^2+b\Delta y_r^2)}{(\Delta x+a^2\Delta x_r)\Delta y}+0.5Pr^*$$
$$(\Delta x^2+a\Delta x_r^2))\omega_{i,j+1}^*+(0.25\beta a_1\frac{(\Delta x^2+a\Delta x_r^2)(\Delta y^2+b\Delta y_r^2)}{(\Delta y+b^2\Delta y_r)\Delta x_r}$$
$$+0.5aPr^*(\Delta y^2+b\Delta y_r^2))\omega_{i-1,j}^*-(0.25\beta a_2$$
$$\frac{(\Delta x^2+a\Delta x_r^2)(\Delta y^2+b\Delta y_r^2)}{(\Delta y+b^2\Delta y_r)\Delta x}-0.5Pr^*(\Delta y^2+b\Delta y_r^2))\omega_{i+1,j}^*$$
$$-(0.25\gamma b_2\frac{(\Delta x^2+a\Delta x_r^2)(\Delta y^2+b\Delta y_r^2)}{(\Delta x+a^2\Delta x_r)\Delta y_r}-0.5bPr^*$$
$$(\Delta x^2+a\Delta x_r^2))\omega_{i,j-1}^*+0.25Pr^*(\Delta x^2+a\Delta x_r^2)(\Delta y^2+b\Delta y_r^2)$$
$$(\frac{S_{1)i+a_2,j}^*-S_{1)i-a_1,j}^*}{(\Delta x_r)^{a_1}(\Delta x)^{a_2}}-\frac{S_{2)i,j+b_1}^*-S_{2)i,j-b_2}^*}{(\Delta y)^{b_1}(\Delta y_r)^{b_2}}-4\frac{S_{3)i+a_2,j}^*-S_{3)i-a_1,j}^*}{(\Delta x_r)^{a_1}(\Delta x)^{a_2}})$$
$$+0.25S_{G)i,j}^*(\Delta x^2+a\Delta x_r^2)(\Delta y^2+b\Delta y_r^2)]$$
$$/[0.5((a+1)(\Delta y^2+b\Delta y_r^2)+(b+1)(\Delta x^2+a\Delta x_r^2))+0.25$$
$$(\Delta x^2+a\Delta x_r^2)(\Delta y^2+b\Delta y_r^2)(\frac{\gamma}{(\Delta x+a^2\Delta x_r)(\Delta y)^{b_1}(-\Delta y_r)^{b_2}}$$
$$+\frac{\beta}{(\Delta y+b^2\Delta y_r)(\Delta x_r)^{a_1}(-\Delta x)^{a_2}})] \qquad (30)$$

$$\theta_{i,j}=[(0.25\gamma b_1\frac{(\Delta x^2+a\Delta x_r^2)(\Delta y^2+b\Delta y_r^2)}{(\Delta x+a^2\Delta x_r)\Delta y}+0.5(\Delta x^2$$
$$+a\Delta x_r^2))\theta_{i,j+1}+(0.25\beta a_1\frac{(\Delta x^2+a\Delta x_r^2)(\Delta y^2+b\Delta y_r^2)}{(\Delta y+b^2\Delta y_r)\Delta x_r}$$
$$+0.5a(\Delta y^2+b\Delta y_r^2))\theta_{i-1,j}-(0.25\beta a_2$$
$$\frac{(\Delta x^2+a\Delta x_r^2)(\Delta y^2+b\Delta y_r^2)}{(\Delta y+b^2\Delta y_r)\Delta x}-0.5(\Delta y^2+b\Delta y_r^2))\theta_{i+1,j}$$
$$-(0.25\gamma b_2\frac{(\Delta x^2+a\Delta x_r^2)(\Delta y^2+b\Delta y_r^2)}{(\Delta x+a^2\Delta x_r)\Delta y_r}-0.5b(\Delta x^2+$$
$$a\Delta x_r^2))\theta_{i,j-1}]/[0.5((a+1)(\Delta y^2+b\Delta y_r^2)+(b+1)$$
$$(\Delta x^2+a\Delta x_r^2))+0.25(\Delta x^2+a\Delta x_r^2)(\Delta y^2+b\Delta y_r^2)$$
$$(\frac{\gamma}{(\Delta x+a^2\Delta x_r)(\Delta y)^{b_1}(-\Delta y_r)^{b_2}}+$$
$$\frac{\beta}{(\Delta y+b^2\Delta y_r)(\Delta x_r)^{a_1}(-\Delta x)^{a_2}})] \qquad (31)$$

An under – relaxation technique can be applied to accelerate the convergence of Eq.(30); the expression is used in this technique presented in the following :

$$\omega_{i,j}^{*k+1}=(1-Fv)\omega_{i,j}^{*k}+(Fv)\omega_{i,j}^*(computed)$$

Where (Fv) is the relaxation factor for the vorticity. The value of this relaxation factor is in the range of (0 to 2) [2].

In order to obtain results of the conservation equations, The above equations (Eqs.(27), (30), and (31)) are subjected to the following boundary conditions [9]:

Case (I) :-

$$0\leq x^*\leq 1 \qquad y^*=0$$
$$\Rightarrow \psi^*=\frac{\partial\psi^*}{\partial y^*}=0 \qquad \frac{\partial\theta}{\partial y^*}=0$$
$$y^*=2x^* \qquad 0\leq x^*\leq 0.5$$
$$\Rightarrow \psi^*=\frac{\partial\psi^*}{\partial x^*}=0 \qquad \theta=1$$
$$y^*=2(1-x^*) \qquad 0.5\leq x^*\leq 1$$
$$\Rightarrow \psi^*=\frac{\partial\psi^*}{\partial x^*}=0 \qquad \theta=0$$

Case (II) :

$$0 \le x^* \le 1 \qquad y^* = 0$$

$$\Rightarrow \psi^* = \frac{\partial \psi^*}{\partial y^*} = 0 \qquad \frac{\partial \theta}{\partial y^*} + 1 = 0$$

$$y^* = 2x^* \qquad 0 \le x^* \le 0.5$$

$$\Rightarrow \psi^* = \frac{\partial \psi^*}{\partial x^*} = 0 \qquad \theta = 0$$

$$y^* = 2(1 - x^*) \qquad 0.5 \le x^* \le 1$$

$$\Rightarrow \psi^* = \frac{\partial \psi^*}{\partial x^*} = 0 \qquad \theta = 0$$

Also, the following finite difference equation for the vorticity at a wall is adopted as the boundary condition for the vorticity equation (see Fig. (2)):

For inclined wall

$$\omega_o = 2\left(\frac{\psi_o - \psi_1}{\Delta x_r^2} + \frac{\psi_o - \psi_2}{\Delta y_r^2}\right)$$

For lower wall

$$\omega_o = \frac{3(\psi_o - \psi_1)}{\Delta x^2} - \frac{\omega_1}{2}$$

The numerical work starts with giving the distributions of stream function and temperature for natural convection as the zeroth-order approximation. Then, obtain the zeroth-order approximation of vorticity: no flow and pure conduction. Based on these old fields, equation (٢٧) is used to determine point-by-point the new (ψ^*) field, and equation (٣٠) is used to determine the new (ω^*), while the energy equation (31) is used to determine the new (θ) field. The iteration process is terminated under the following condition:

$$\sum_{i,J} \left| \tau^{r+1}{}_{i,j} - \tau^{r}{}_{i,j} \right| \Big/ \sum_{i,J} \tau^{r+1}{}_{i,j} \le 10^{-5} \qquad (32)$$

where, (τ) stands for either ($\psi^*, \omega^*, or \theta$); (r) denotes the iteration step.

Before starting the computational solution, the grid independence of the results must be tested. Thus, numerical experiments have been carried out to solve a two – dimensional convection problem in which the non – dimensional parameter (NE = 0). The modified Prandtl number in this test is set to be (6.7), while the grid size varies from (10×10) to (60×60) for different values of modified Rayleigh number as shown in Fig.(5). It is found that the change in the Nusselt number for grid size of (35×35) and (45×45) is less than (0.9) percent for the range of modified Rayleigh number ($10^3 \le Ra_E \le 10^5$). Therefore, the number of grid that is adopted in the present study is (35×35) for all four cases. The number of grid was selected as a compromise between accuracy and speed of computation.

4. Results And Discussion :-

Case (I) :- Triangular enclosure under B.C.1

a-Temperature and Flow Fields:

The contour lines of the temperature distribution and flow fields for different values of system parameters are presented in Figs.(6) to (9). For conduction regime (i.e. at $Ra_E < 10^3$ and $NE < 1$), the isotherms are almost straight lines. However, the buoyancy induced flow at $Ra_E \ge 10^3$ or $NE \ge 1$ changes the direction of the isotherms, and, as a result, clockwise convective motion is formed, as shown in Figs.(6 & 8). It is observed that as the Ra_E or NE increases more, isotherms shift

g.(7). The shift is

more pronounced as the Ra_E increase more and more, as shown in Fig.(9). This results in the asymmetry of the temperature field in the core. It can also be seen that as Ra_E or NE increases, the change in temperature with respect to height, reduces in the lower portion of the enclosure, but increases faster in the upper portion. Furthermore, the temperature gradient near the hot wall increases rapidly as the Ra_E increases. The behavior is just the reverse near the cold wall.

For a given Pr^* and NE, an increase in Ra_E results in a thicker cold layer near the bottom wall and a high temperature field near the top edge (Figs.(7a & 9a).

The growth of the boundary layers on the inclined walls are also observed to be affected by a variation in Ra_E, Pr^* and NE. The increase in NE at a fixed Ra_E is seen to increase the rate of boundary layer growth on the hot wall. This behavior is reversed on the cold wall. The net result is a shift of the core toward the cold wall and toward the top edge of the heated wall. This shift is further strengthened if there is an increase in Ra_E or NE. Generally higher convective velocities in the lower left – hand corner are produced as a result of the shift. Also, the horizontal velocity in the upper region is much higher as compared to that in the lower region for increased values of Ra_E or NE.

Fig.(10) represents the variation of $\psi_{\max}$ with Ra_E for different values of NE and Pr^*=10. It is seen that the value of ψ_{max} increases and reaches the peak value at $Ra_E = 10^5$, for NE =10.

Fig.(8a) shows the streamlines at Ra_E=10^5, Pr^* = 1 and NE =0. The flow consists of one large cell rotating in the enclosure. It also shows the flow slowly rises along the heated wall, turning the edge at the top of the enclosure, and slowly slides along the cooled wall.

b-Heat Transfer Coefficient:

To understand the heat transfer process by natural convection, it must be to evaluate the heat transfer coefficient (h), but to make the present work having generality, the calculated results must be in dimensionless form. Therefore, it must be needed to evaluate Nusselt number (Nu) as a function of influence parameters. Fig.(11) shows the variation of Nu_a versus Ra_E with different values of NE and Pr^*=10 on the hot wall of the enclosure. It is clear that Nu_a equal to (3.253) in the conduction regime. This is mainly due to the very small distance between the isothermal walls in the upper region of the triangular enclosure, which allow more heat flow rate to transfer along it. Also, the depth of the layer is thin and the slope of the inclined wall is large. It is also seen that for range of modified Rayleigh number before (10^3), the rate of increase in Nu_a against Ra_E for different values of NE and a fixed Pr^* is relatively small. But, Nu_a increases rapidly as NE increases for $Ra_E \geq 10^3$ expressing the increase of convective heat transfer. It is also noticed that

the effect of NE on Nu_a is more pronounced as the Ra_E numbers increase.

Case (II) :- Triangular enclosure under B.C.2

a-Temperature and Flow Fields:

Figs.(12) to (17) show the contour lines of the temperature distribution and flow fields for the present case.

For low Ra_E^*, the isotherms in the lower region are almost parallel for a large part of the inclined wall indicating that a substantial amount of energy is rejected on this part when the Ra_E^* is small. However, the heat transfer on this surface decreases with an increase in Ra_E^* which clearly implies that the effect of the lower portion boundary condition diminishes with higher velocities or higher Ra_E^*, as shown in Figs.(13 & 15).

As the Ra_E^* or NE increases, the temperature in the lower portion of the enclosure decreases while that in the upper region increases. The stratification in the upper layers is, thus, more strength than that occurs in case (I) as show in Figs.(9d) and (17d), this because of the change in the boundary condition at enclosure walls from (B.C.1) to (B.C.2), which allow less heat flow rate to transfer along the lower part of isothermal wall.

As Ra_E^* increase more, or NE increase for high values of Ra_E^*, results in the stable of the stratification area near the top edge and decreased θ_{max} respectively. In Fig.(15d), the isotherms become parallel for large part of inclined wall in the upper region indicating that a large amount of energy is rejected [illegible] and more, or NE increase for high values of Ra_E^* the temperature and flow field modified, and the stratification layer concentrated in the small region near the top edge of the enclosure, as presented in Fig.(17d).

The natural of the convection cell, Initially (i.e. at $Ra_E^* = 10$) the flow consists of a single cell filling the entire enclosure and rotating slowly in the clockwise direction. However, an increase in Ra_E^* or NE results in changing the flow pattern from unicellular to multicellular flow. Fig.(16d) shows the streamlines at $Ra_E^* = 10^5$, $NE = 1$, and $Pr^* = 10$. This flow exhibits two counter – rotating cells, each covering half of the enclosure. Both components have the same maximum magnitude ($\psi_{max} = 14.2$), but are of opposite sign indicating an opposite direction of flow. These two cells are symmetric about the center line of the enclosure. The convective velocity near the wall is lower than that along the line of symmetry. Fig.(18) represents the variation of ψ_{max} with Ra_E^* for different values of NE and Pr^*=10.

Furthermore, the isotherms are symmetric about the vertical line at $x = 0.5$, and the maximum temperature always occurs at the middle of the lower wall, and is a function of Ra_E^*, NE, and Pr^*.

b-Heat Transfer Coefficient:

The average Nusselt number as defined by Eq.(26) is presented in Fig.(19). It [illegible] that for Ra_E^* and NE are less than

(10^4) and (1) respectively, the rate of increase in Nu_a is relatively small. Then, Nu_a increases rapidly as Ra_E^* or NE increases expressing the existence and increase of convective heat transfer. As already indicated by the temperature field, the average Nusselt number for the present case is higher than that for the case (I) for the same given condition.

Finally, Four correlation equations have been predicted depending on variation of modified Rayleigh number, modified Prandtl number, and non – dimensional parameter of the Prandtl – Eyring model for both two cases, by using least square method.

Case (I): Triangular enclosure under B.C.1

$$Nu_a = 1.672\, Ra_E^{0.0962}\, Pr^{*\,0.0237}\, (NE+1)^{1.47},$$
$$0 \le NE \le 0.1, \quad R = 0.8891 \qquad (33)$$

and,

$$Nu_a = 1.512\, Ra_E^{0.119}\, Pr^{*\,0.0671}\, (NE+1)^{0.0205},$$
$$0.1 < NE \le 10, \quad R = 0.9621 \qquad (34)$$

Case (II): Triangular enclosure under B.C.2

$$Nu_a = 2.855\, Ra_E^{*0.0901}\, Pr^{*\,0.0098}\, (NE+1)^{1.036},$$
$$0 \le NE \le 0.1, \quad R = 0.874 \qquad (35)$$

and,

$$Nu_a = 1.677\, Ra_E^{*0.149}\, Pr^{*\,0.0899}\, (NE+1)^{0.0699},$$
$$0.1 < NE \le 10, \quad R = 0.9592 \qquad (36)$$

The above correlations are acceptable in the range of modified Rayleigh number (10^2 to 10^5), modified Prandtl number (1 to 100), and non – dimensional parameter (NE= 0 to 10).

To ensure that these approximation correlations are usable, the coefficient of determination (R) had been obtained for each equation. The minimum value of (R) was (0.874), that means these approximate equations are good for predicting the value of average Nusselt number. Figs.(20) and (21) show the comparison between numerical and predicted results. Agreement between numerical and predicted is close, although most the predicted points lie near the theoretical line.

٥. Conclusions :-

The main conclusions of the present work are:

1- For the two cases that have been solved, it has been demonstrated that the average Nusselt number is a strong function of modified Rayleigh number, non – dimensional parameter (NE), and modified Prandtl number, also the results show the average Nusselt number:

a- Increases as (Ra) increases, for a given values of (NE) and (Pr*).

b- Increases as (NE) increases except for (NE > 0.1) at ($Ra \ge 10^5$), for a given value of (Pr*).

c- Nu_a for the second case of thermal boundary conditions (B.C.2) is always higher than for the first case (B.C.1).

2- For large modified Rayleigh number, the non – dimensional parameter (NE) of the Prandtl – Eyring model has, for a given modified Rayleigh and Prandtl numbers, a large effect on the heat transfer rate, while for small (Ra), it does not have much effect on

the heat transfer because in this situation, the convection is very weak and the dominant mode of energy transfer is conduction.

3- In the first case of the boundary conditions (B.C.1), the flow is mainly single cell flow, while in the second case (B.C.2), the flow consist of two counter-rotating cells, each covering half of the enclosure.

References :

[1] Elba, O. B., Julio, C. R., and Obidio, R., "Numerical Simulation for the Natural Convection Flow", Numerical methods in Fluids, Vol. 30, PP. 237-254, 2000.

[2] Nabeel, M., "A Numerical Study of Natural Convection Heat Transfer in an Enclosure for Newtonian and Non - Newtonian Fluids", M. Sc. Thesis, University of Kufa , 2005.

[3] Miomir, R., "Numerical Investigation of Laminar Natural Convection in Inclined Square Enclosures", Physics, Chemistry and Technology, Vol. 2, PP.149-157, 2001.

[4] J. M. Coulson, and J. S. Richardson, "Chemical Engineering", Bergamon, International Library, Vol. 3, 1983.

[5] Myers, E., "Analytical Methods in Conduction Heat Transfer", Mc Graw – Hill Book Company, Inc., 1971.

[6] Frank, K., and Mark, S., "Principles of Heat Transfer", 5th Edition, PWS Publishing Company, 1997.

[7] Bejan, A., "Convection Heat Transfer", Wiley, Inter Science Publication, John Wiley and Sons, Inc., 1984.

[8] Najdat N., "Laminar Flow Separation in Constructed Channel", Ph.D. Thesis, Michigan State University, 1987.

[9] G., Lauriat, "Numerical Study of the Interaction of Natural Convection with Radiation in Nongray Gases in a Narrow Vertical Cavity", Int. Journal of Heat Transfer, Vol. 2, PP. 153-158, 1982.

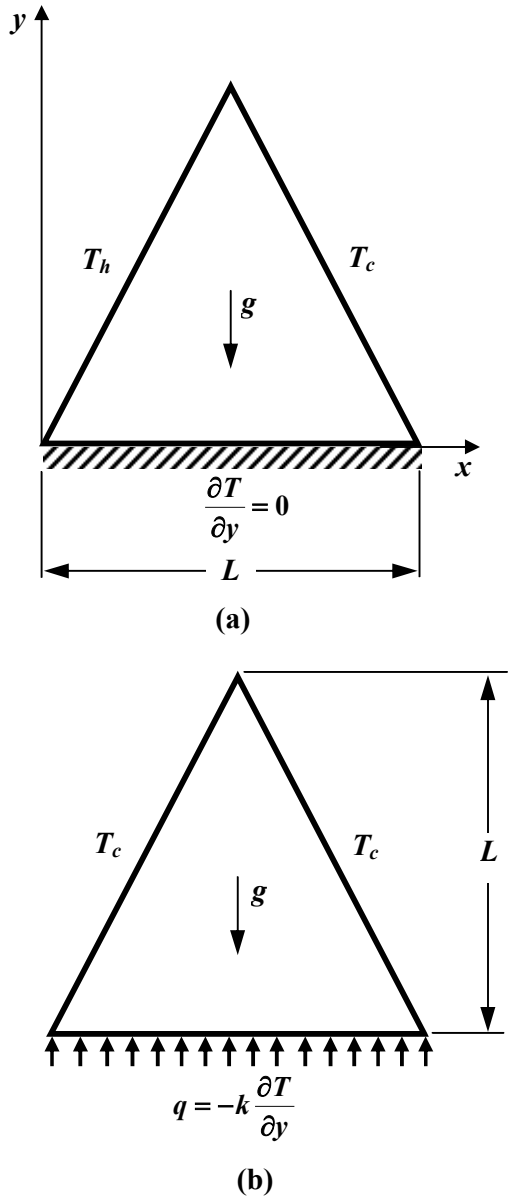

Fig.(1) Physical model and coordinate system.

(a) case (I), (b) case (II)

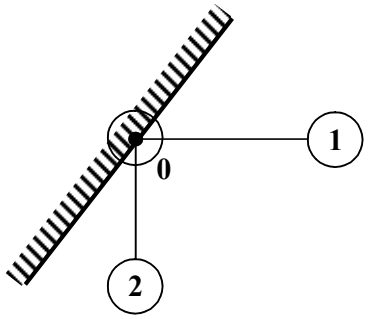

Fig.(2) Nodes used to obtain vorticity at the inclined wall.

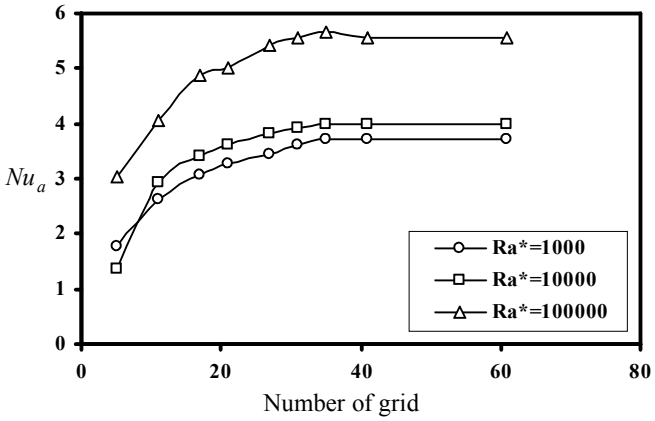

Fig.(5) Variation of Nusselt number with the number of grid points for different modified Rayleigh number. Case (I) .

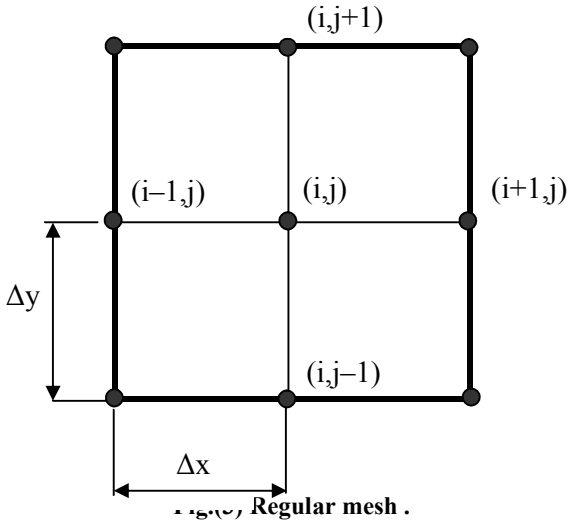

Fig.(3) Regular mesh .

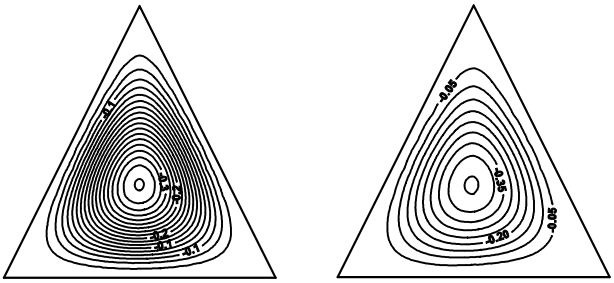

(a) **(b)**

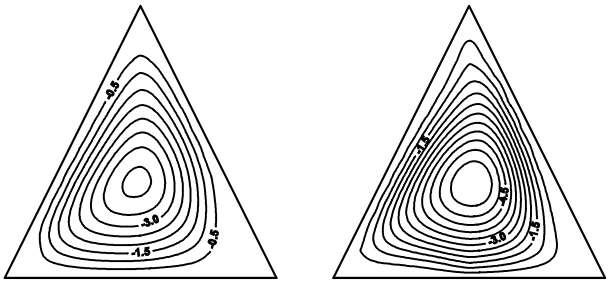

(c) **(d)**

Fig.(6) Pattern of streamlines for Ra_E =10^3 and Pr^*=10. (a) *NE*=0, (b) *NE*=0.1, (c) *NE*=1, (d) *NE*=10. Case (I)

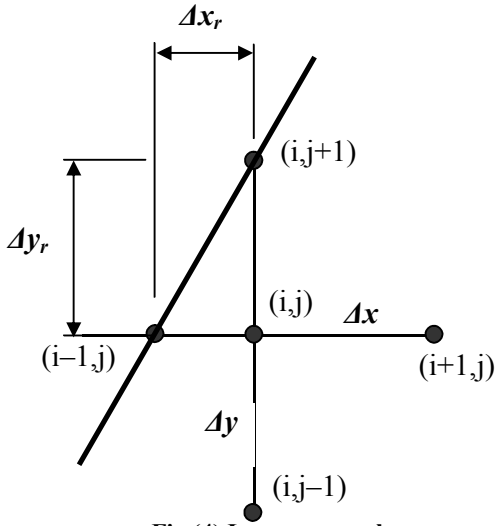

Fig.(4) Irregular mesh.

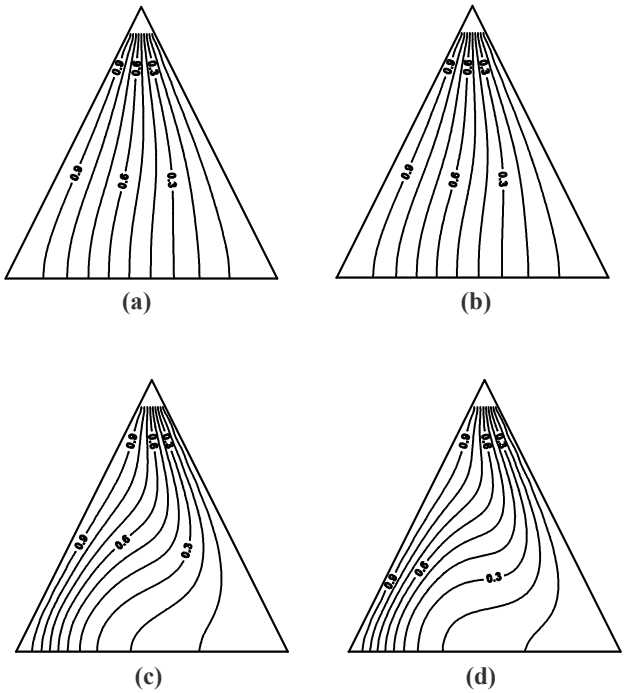

Fig.(7) Pattern of isotherms for Ra_E =10^3 and Pr^*=10. (a) NE=0, (b) NE=0.1, (c) NE=1, (d) NE=10. Case (I)

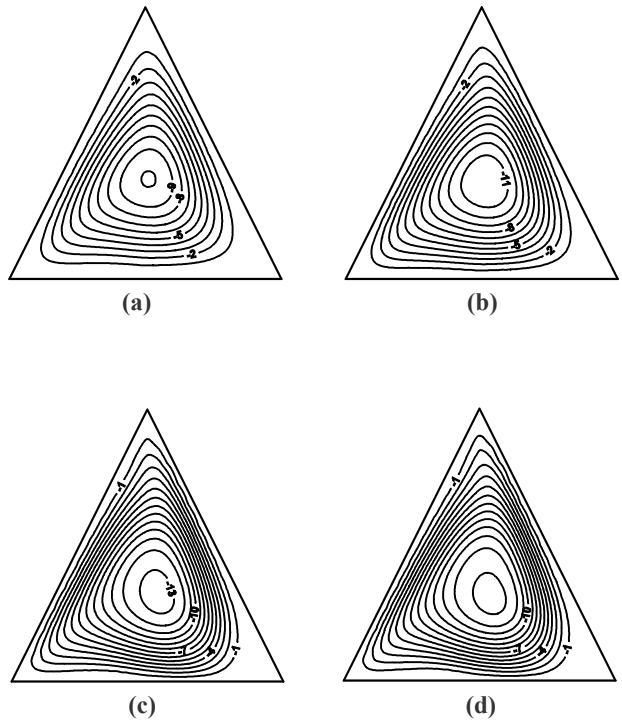

Fig.(8) Pattern of streamlines for Ra_E =10^5 and Pr^*=1. (a)NE=0, (b)NE=0.005, (c)NE=0.05, (d)NE=0.1. Case (I)

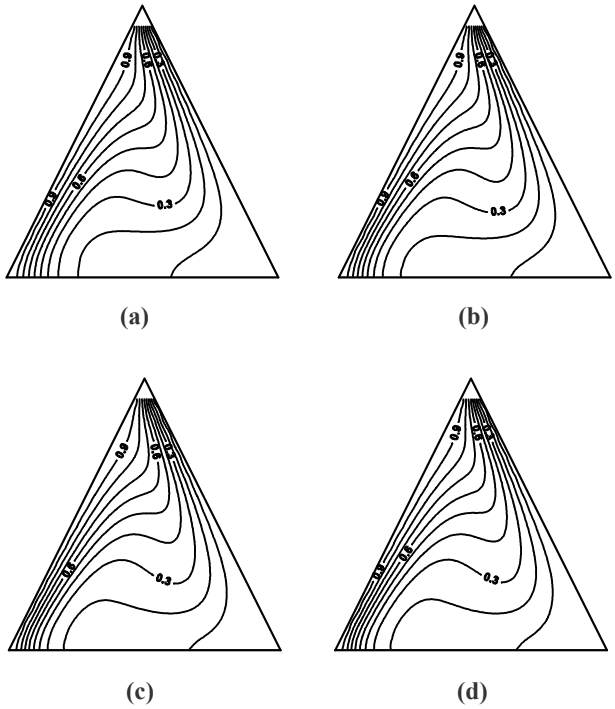

Fig.(9) Pattern of isotherms for Ra_E =10^5 and Pr^*=1. (a)NE=0, (b)NE=0.005, (c)NE=0.05, (d)NE=0.1. Case (I)

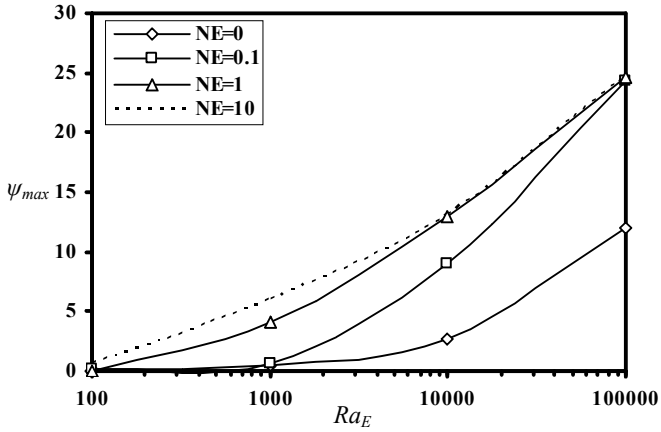

Fig.(10) Variation of $(\psi)_{\max}$ with the Ra_E for different values of NE and Pr^*=10. Case (I)

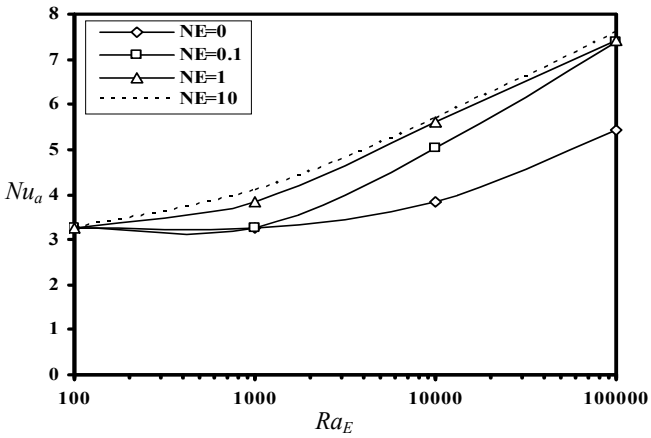

Fig.(11) Variation of Nu_a with the Ra_E for different values of *NE* and *Pr=10. Case(I)**

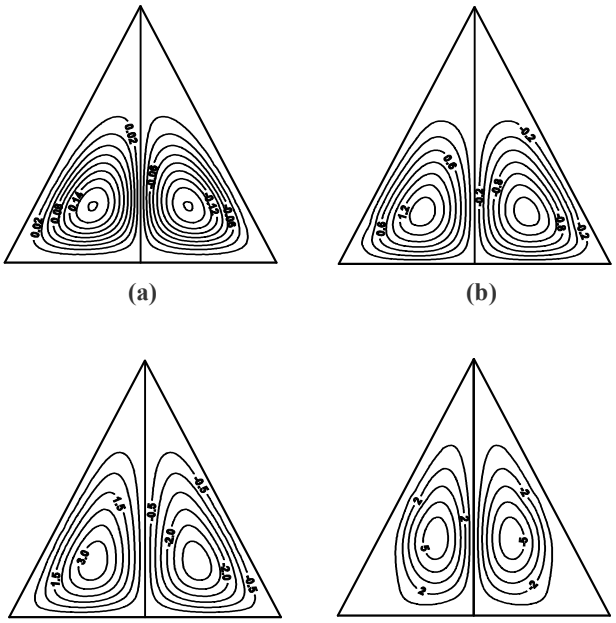

(a) (b) (c) (d)

Fig.(12) Pattern of streamlines for Ra^*_E =10^4 and Pr^*=10. (a) *NE*=0, (b) *NE*=1, (c) *NE*=6, (d) *NE*=10. Case (II)

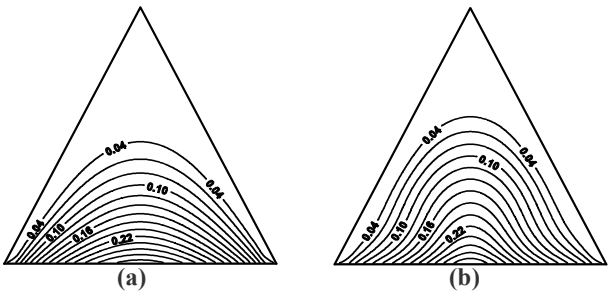

(a) (b)

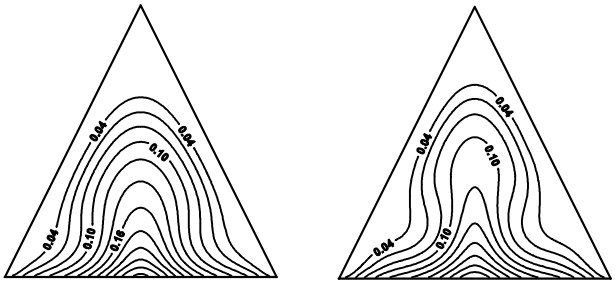

(c) (d)

Fig.(13) Pattern of isotherms for Ra^*_E =10^4 and Pr^*=10. (a) *NE*=0, (b) *NE*=1, (c) *NE*=6, (d) *NE*=10. Case (II)

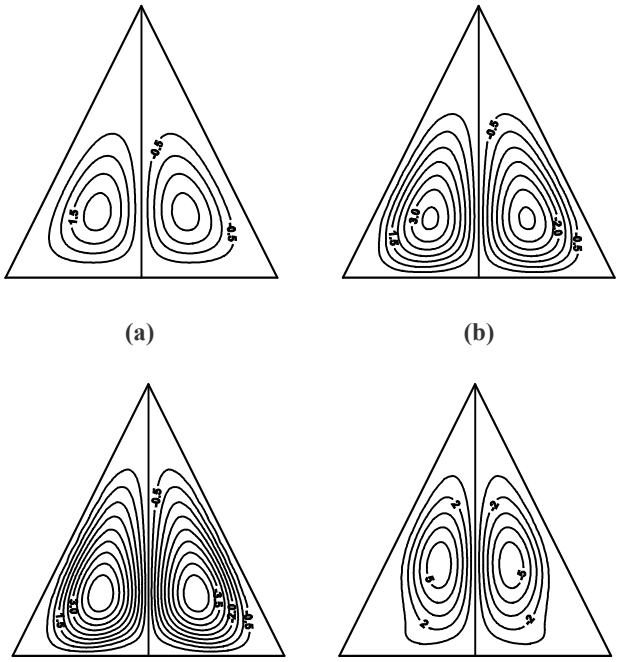

(a) (b) (c) (d)

Fig.(14) Pattern of streamlines for Ra^*_E =10^5 and Pr^*=1. (a) *NE*=0, (b) *NE*=0.1, (c) *NE*=0.5, (d) *NE*=1. Case (II)

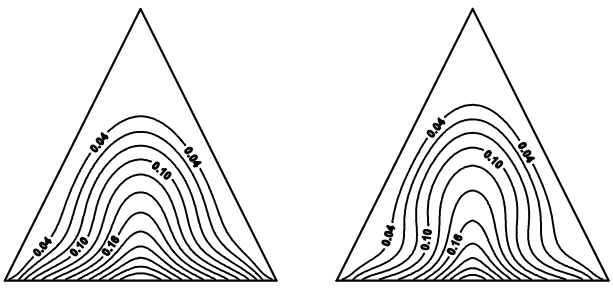

(a) (b)

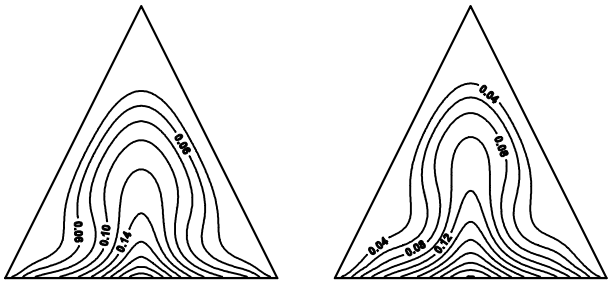

(c) (d)

Fig.(15) Pattern of isotherms for Ra^*_E =10^5 and Pr^*=1. (a) *NE*=0, (b) *NE*=0.1, (c) *NE*=0.5, (d) *NE*=1. Case (II)

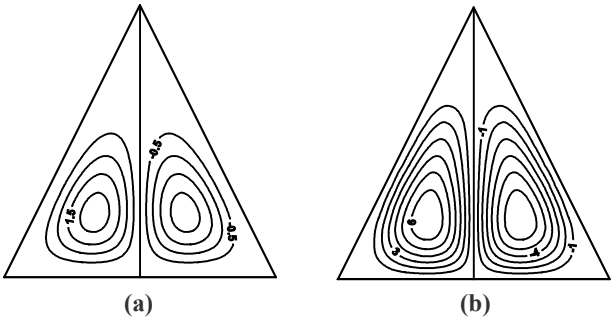

(a) (b)

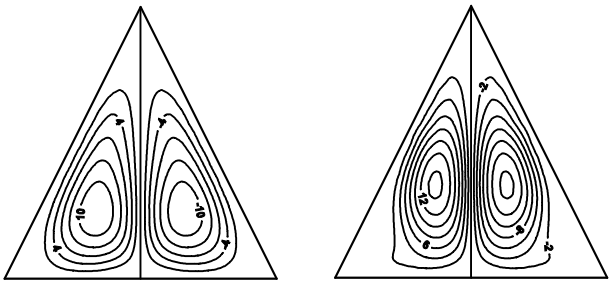

(c) (d)

Fig.(16) Pattern of streamlines for Ra^*_E =10^5 and Pr^*=10.(a)*NE*=0,(b)*NE*=0.1,(c)*NE*=0.5,(d)*NE*=1.Case(II)

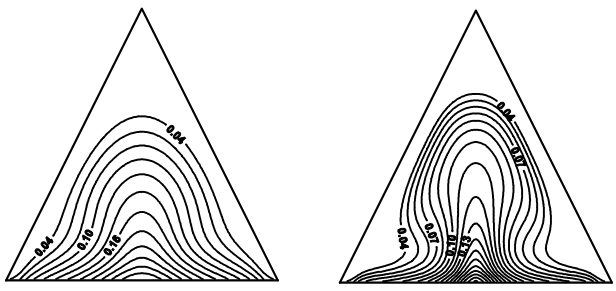

(a) (b)

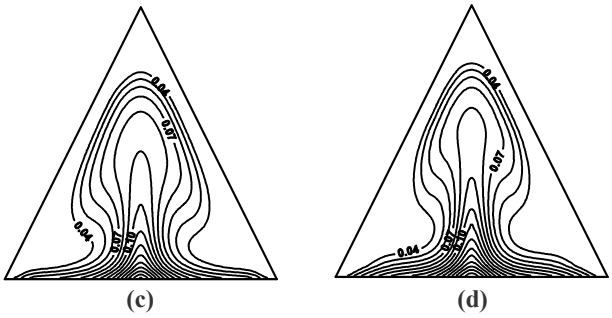

(c) (d)

Fig.(17) Pattern of isotherms for Ra^*_E =10^5 and Pr^*=10. (a) *NE*=0, (b) *NE*=0.1, (c) *NE*=0.5, (d) *NE*=1. Case (II)

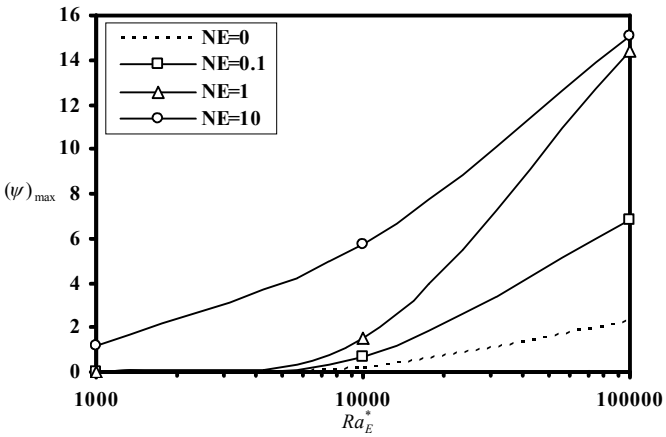

Fig.(18) Variation of $(\psi)_{max}$ with the R^*_E for different values of *NE* and *Pr=10. Case(II)**

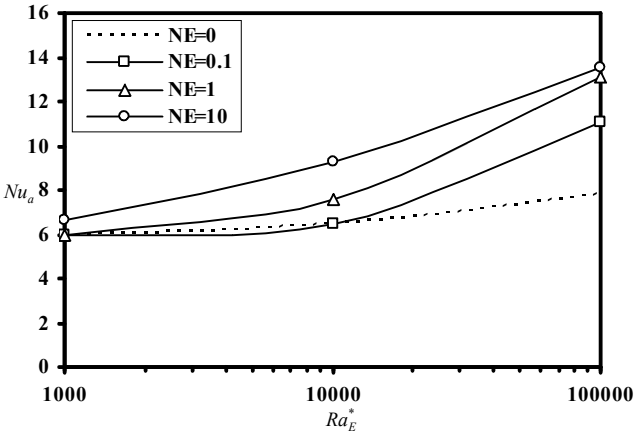

Fig.(19) Variation of Nu_a with the R^*_E for different values of *NE* and *Pr=10. Case(II)**

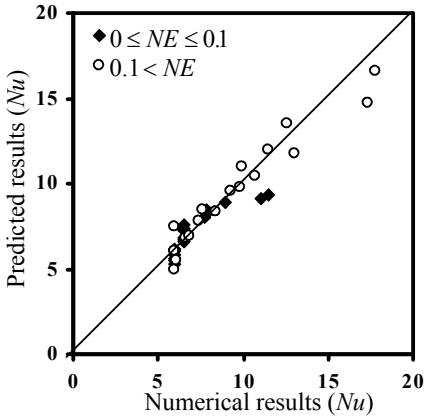

Fig.(20) Numerical results vs. Predicted results of correlation equation. Case (I)

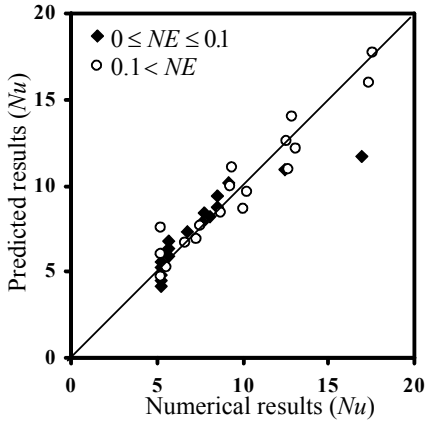

Fig.(21) Numerical results vs. Predicted results of correlation equation. Case (II)

انتقال الحرارة بالحمل الطبيعي الطباقي لموائع نيوتونية وغير نيوتونية في وسط مغلق مثلث الشكل

د.علاء عباس مهدي
كلية الهندسة – جامعة الكوفة
قسم الهندسة الميكانيكية

الخلاصـــــــة :

في هذا البحث إجراء دراسة عددية لانتقال الحرارة بالحمل الطبيعي الطباقي الثنائي البعد لموائع نيوتونية وغير نيوتونية في وسط مغلق مثلث الشكل ضمن مدى واسع لعدد رالي المحور ($10^2 \le Ra \le 10^5$) وللمقدار اللا بعدي للموديل الرياضي (Prandtl – Eyring) يمتد من ($0 \le NE \le 10$) ولعدد برانتل المحور أخذ في المدى (Pr^* =1,10, and 100). افترض نوعان من الظروف الحدية. الأول, عندما تكون الجدران المائلة مسخنة إلى درجات حرارة مختلفة ومنتظمة والجدار السفلي معزول. الثاني, عندما يكون الجدار السفلي مسخن بمصدر حراري ثابت بينما الجدران المائلة عند درجة حرارة منخفضة وثابتة. كذلك افترض بأن سلوك الموائع غير– نيوتونية يخضع للموديل الرياضي (Prandtl – Eyring). تم تمثيل نتائج الدراسة بدلالة خطوط درجات الحرارة الثابتة وخطوط الانسياب لبيان سلوك درجة الحرارة والجريان في الحيز. بالإضافة إلى رسومات بيانية أخرى تمثل علاقة معدل عدد نسلت مع المتغيرات المذكورة أعلاه. إن الدراسة الحالية بينت تأثير المقدار اللا بعدي (NE) على السرعة ودرجة الحرارة. كذلك بينت إن عدد نسلت هو دالة قوية من عدد رالي المحور وعدد برانتل المحور والمقدار اللا بعدي (NE) والظروف الحدية. تم إيجاد علاقات تقريبية تمثل اعتمادية معدل عدد نسلت على عدد رالي المحور وعلى عدد برانتل المحور والمقدار اللا بعدي (NE).